energy&fuels

Article

pubs.acs.org/EF

Investigation of Combined Supports for Cu-Based Oxygen Carriers for Chemical-Looping with Oxygen Uncoupling (CLOU)

Iñaki Adánez-Rubio,[†] Mehdi Arjmand,[*,‡] Henrik Leion,[‡] Pilar Gayán,[†] Alberto Abad,[†] Tobias Mattisson,[§] and Anders Lyngfelt[§]

[†]Instituto de Carboquímica (ICB-CSIC), Department of Energy & Environment, Miguel Luesma Castán, 4, Zaragoza, 50018, Spain

[‡]Department of Chemical and Biological Engineering, Division of Environmental Inorganic Chemistry, Chalmers University of Technology, SE-412 96 Göteborg, Sweden

[§]Department of Energy and Environment, Division of Energy Technology, Chalmers University of Technology, SE-412 96 Göteborg, Sweden

ABSTRACT: The chemical-looping with oxygen uncoupling (CLOU) process is a novel solution for efficient combustion with inherent separation of carbon dioxide. The process uses a metal oxide as an oxygen carrier to transfer oxygen from an air to a fuel reactor. In the fuel reactor, the metal oxide releases gas phase oxygen, which oxidizes the fuel through normal combustion. In this study, Cu-based oxygen carrier materials that combine different supports of $MgAl_2O_4$, TiO_2, and SiO_2 are prepared and characterized with the objective of obtaining highly reactive and attrition resistant particles. The oxygen carrier particles were produced by spray-drying and were calcined at different temperatures ranging from 950 to 1030 °C for 4 h. The chemical-looping performance of the oxygen carriers was examined in a batch fluidized-bed reactor in the temperature range of 900−950 °C under alternating reducing and oxidizing conditions. The mechanical stability of the oxygen carriers was tested in a jet-cup attrition rig. All of the oxygen carriers showed oxygen uncoupling behavior with oxygen concentrations close to equilibrium. During reactivity tests with methane, oxygen carriers with lower mechanical stability showed higher reactivity, yielding almost complete fuel conversion. Oxygen carrier materials based on support mixtures of $MgAl_2O_4/TiO_2$, $MgAl_2O_4/SiO_2$, and TiO_2/SiO_2 showed a combination of high mechanical stability, low attrition rates, good reactivity with methane, and oxygen uncoupling behavior.

1. INTRODUCTION

The intergovernmental panel on climate control (IPCC) has suggested that a 50−85% reduction in total CO_2 emission is necessary by 2050 to restrict the predicted global temperature rise to 2 °C.[1] In order to mitigate the increasing levels of carbon dioxide in the atmosphere, several technologies have been proposed. Among suggested alternatives, one solution is to reduce the CO_2 emissions in combustion processes by means of a scheme, generally called Carbon Capture and Storage (CCS). However, the greatest drawback with most of the proposed processes is that there are large costs and energy penalties incurred due to gas separation steps needed in order to obtain CO_2 in a pure form. Consequently, the overall efficiency of the power generation process may decrease by approximately 7−15%, when using conventional capture techniques in comparison to combustion without carbon capture. One solution for this problem is chemical-looping combustion (CLC).[2]

The principle concept of the chemical-looping combustion process is based on two interconnected reactors, an air and a fuel reactor, with an oxygen carrier circulating between them.[3−5] The scheme of the CLC process is shown in Figure 1. When fuel and air are introduced into the respective reactors, the following reactions occur, i.e., reaction 1 in the fuel reactor and reaction 2 in the air reactor:

$$(2n + m)Me_xO_y + C_nH_{2m} \rightarrow (2n + m)Me_xO_{y-1} + nCO_2 + mH_2O \quad (1)$$

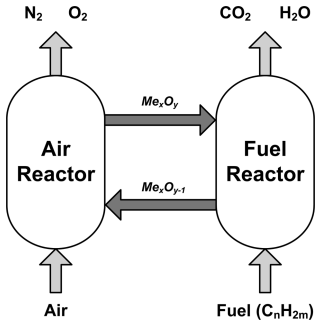

Figure 1. Schematic of the chemical-looping combustion (CLC) process.

$$2Me_xO_{y-1} + O_2 \rightarrow 2Me_xO_y \quad (2)$$

Here, Me_xO_y and Me_xO_{y-1} are the oxidized and the reduced forms of an oxygen carrier. C_nH_{2m} is the fuel, which could be gas, liquid, or solid. In the event of complete fuel conversion, the exhaust stream from the fuel reactor would ideally consist of only CO_2 and water steam, from which pure CO_2 could be obtained after condensing the water. The reduced oxygen carrier (Me_xO_{y-1}) would then be circulated back to the air reactor to reoxidize with air, thus becoming ready for the next cycle. The reaction in the fuel reactor can be either endothermic or exothermic depending on the fuel and the oxygen carrier;

Received: April 16, 2013
Published: June 24, 2013

however, the oxidation of the oxygen carrier in the air reactor is always exothermic.[6] By combining the reduction, eq 1, with the oxidation, eq 2, it is seen that the overall reaction becomes identical with the conventional combustion process, which shows that the CLC process does not entail any direct energy penalty for CO_2 separation.

The chemical-looping combustion (CLC) process was initially introduced by Lewis and co-workers[7] to produce a pure stream of CO_2. In 1994, Ishida and Jin[8] suggested that this technique could be used for CO_2-capture from power plants. In 2001, Lyngfelt et al.[3] proposed a unit consisting of two interconnected fluidized-bed units to implement the chemical-looping combustion process. The process was first demonstrated for gaseous fuels in 2003.[9] Later, Kolbitsch et al.[10] designed, built, and operated a 120 kW unit consisting of two circulating fluidized bed reactors. To date, CLC has been successfully demonstrated in a number of units of sizes up to 120 kW[11] and overviews of current achievements in CLC are given by Lyngfelt,[11,12] Hossain and de Lasa,[13] and Adanez et al.[14]

In general, the use of solid fuels, such as coal, in CLC requires one more step than the combustion of gaseous fuels. Solid fuel conversion through direct solid−solid contact between the oxygen carrier and the fuel is not expected to occur at an appreciable rate. Hence, there are two options for using solid fuels in this case, CLC with gasification of solid fuels[15] and chemical-looping with oxygen uncoupling (CLOU).[16] The first approach involves gasifying the char that remains after devolatilization in the presence of steam, which produces CO and H_2. These gases can then react with the oxygen carrier to produce CO_2 and H_2O similar to eq 1. However, in the case of CLOU, an oxygen carrier provides gaseous oxygen during the reduction phase, according to eq 3, and the char reacts directly with the uncoupled gaseous oxygen:

$$Me_xO_y \rightarrow Me_xO_{y-2} + O_2 \quad (3)$$

The reduced oxygen carrier is then transferred to the air reactor for reoxidation. The overall heat of reaction for the CLOU process is the same as for CLC, and only the mechanism by which the fuel accesses the oxygen in the carrier is different. Furthermore, the CLOU process benefits from avoiding the slow gasification of the solid fuel that is needed to produce the synthesis gas that can react with the oxygen carrier.[16] It should be emphasized that the oxygen carrier in CLOU must be able to both react with O_2 (oxidize) and release O_2 at temperatures suitable for the process, i.e., 800 to 1200 °C.

The most commonly proposed approach to realizing CLC is to use interconnected fluidized-bed reactors in a fashion similar to the circulating fluidized-bed boiler (CFB),[3] the difference being that CLC will require an active oxygen carrier rather than inert sand as the bed material. Conventional CFB boilers often operate at an air to fuel ratio of about 1.2, which in the case of CLC corresponds to an outlet oxygen concentration from the air reactor close to 5%. It is important to note that this concentration is somewhat higher than in normal combustion since the flue gas from the air reactor does not contain CO_2. As a result of this, oxide systems with an equilibrium oxygen partial pressure lower than 5% at temperatures typical of the air reactor are desirable. Otherwise, a higher air ratio than in the conventional combustion process will be required, which would result in a higher heat loss due to a larger flue gas stream. Moreover, the oxygen carrier should also be able to release a sufficiently large amount of oxygen in the fuel reactor and at a sufficiently high rate. Thus, the choice of oxygen carriers for the CLOU process is limited by these kinds of considerations. Demonstration of the CLOU process[17] has proven the advantage of this technology over the CLC process, where slow gasification is an imperative step.[18] Moreover, the solids inventory in the fuel reactor of the CLOU process would be lower than in CLC,[19,20] which means avoiding the need for a carbon stripper for reaching a high CO_2 capture rate.[20]

An essential aspect in the development of the CLC and the CLOU processes is the selection of oxygen carrier materials with reasonable reactivity. Oxygen carriers consisting of oxides of transition metals (Mn, Fe, Co, Ni, and Cu), their mixtures, and a number of natural minerals (ores), industrial wastes, and byproducts have been investigated in CLC and CLOU.[11−14] In general, important characteristics of the oxygen carriers are reactivity during oxidation and reduction over a large number of cycles and the ability to fully convert the fuel. Furthermore, thermal and mechanical stability, proper fluidization characteristics, and resistance to attrition and agglomeration are sought-after properties. One way of achieving these properties in oxygen carriers is to combine the active phase (carrier oxide) with an inert support such as TiO_2, SiO_2, ZrO_2, Al_2O_3, or $MgAl_2O_4$ during particle fabrication and/or heat-treating the oxygen carriers.[13]

Considerable attention has been given to copper-oxide materials as efficient oxygen carriers, owing to their high oxygen transport capacity, high reactivity, and absence of thermodynamic limitation, for the complete conversion of the fuel.[11−14] Among various investigated supports for CuO oxygen carriers, Al_2O_3 has been extensively used.[21−32] However, when Al_2O_3 is used as the support, there is a facile interaction between CuO and Al_2O_3, during either fabrication or operation, which results in the partial loss of CuO and CLOU behavior due to the formation of copper(II) aluminate ($CuAl_2O_4$) and copper(I) aluminate ($CuAlO_2$; delafossite) phases.[21−32] Since the copper-aluminate phases are highly reducible,[21−32] this interaction does not necessarily create any obstacle with respect to CLC application. For application in CLOU, however, this interaction should be hindered in order to preserve CuO as the active phase, for instance by using other supports such as TiO_2, ZrO_2, SiO_2, or $MgAl_2O_4$.

Most of the studies using Cu-based oxygen carriers have been carried out at low temperatures (~800 °C) where the CLOU effect is minor, i.e., the application for CLC.[11−14] However, at higher temperatures (~950 °C), an increase in the carbon conversion rate in the presence of CuO particles has been reported and has been associated with the direct oxidation of char.[7] It is now well established that CuO decomposes to Cu_2O when the actual concentration of oxygen is lower than the equilibrium concentration.[16] Consequently, oxygen is released, which allows CLOU to take effect. For temperatures of 900 and 925 °C, this occurs at oxygen concentrations below 1.5 and 2.7%, respectively.[16] Thus, from a CLOU point of view, the optimum temperature of the air reactor is most likely in the range of 900 to 925 °C for Cu-based oxygen carriers. Research has also been conducted on Cu-based oxygen carriers in the temperature regime applicable for CLOU in fluidized-bed batch reactors,[16,19,20,23,33−39] continuous operations,[17,34,40,41] and thermogravimetric studies,[35,42−44] with and without supports.

The major issue in the development of Cu-based oxygen carriers for CLOU has been the mechanical stability of the carriers during continuous operation. One suitable and often-used criterion for characterizing the mechanical integrity of oxygen carriers has been the crushing strength (CS), i.e., the

dx.doi.org/10.1021/ef401161s | Energy Fuels 2013, 27, 3918−3927

Table 1. Oxygen Carriers Prepared in This Work

oxygen carrier[a]	active phase (content [wt %])	support phase (content [wt %])	crushing strength (CS) [N]	comments
C4T6_950			3.2	
C4T6_970		TiO_2 (60)	4.1	
C4T6_1000			—	formation of melt
C4MA6_1000		$MgAl_2O_4$ (60)	0.6	
C4MA6_1030			0.8	
C4S6_1000		SiO_2 (60)	0.7	
C4S6_1030			0.5	
C4MA4T2_970			1.0	
C4MA4T2_1000		$MgAl_2O_4$ (40), TiO_2 (20)	1.5	
C4MA4T2_1030			—	formation of melt
C4MA2T4_970			1.3	
C4MA2T4_1000		$MgAl_2O_4$ (20), TiO_2 (40)	1.0	
C4MA2T4_1030			—	formation of melt
C4MA4S2_970	CuO (40)		—	formation of soft particles
C4MA4S2_1000		$MgAl_2O_4$ (40), SiO_2 (20)	1.4	
C4MA4S2_1030			1.7	
C4MA2S4_1000		$MgAl_2O_4$ (20), SiO_2 (40)	—	formation of soft particles
C4MA2S4_1030			—	
C4T4S2_950			1.7	
C4T4S2_970		TiO_2 (40), SiO_2 (20)	1.8	
C4T4S2_1000			—	formation of melt
C4T2S4_1000		TiO_2 (20), SiO_2 (40)	1.1	
C4T2S4_1030			1.0	
C4MA2T2S2_950			—	
C4MA2T2S2_970		$MgAl_2O_4$ (20), TiO_2 (20), SiO_2 (20)	—	
C4MA2T2S2_1000			—	formation of melt
C4MA2T2S2_1030			—	

[a]Example of nomenclature for the oxygen carriers. C4MA4T2_1000: C4, 40 wt % CuO; MA4, 40 wt % $MgAl_2O_4$; T2, 20 wt % TiO_2; 1000, sintering temperature [°C].

force needed to fracture a single particle. Oxygen carriers with a crushing strength above 1 N have generally shown better performance with respect to attrition in continuous operation. A recent investigation has shown that oxygen carrier particles with a crushing strength above 2 N are more likely to resist attrition than softer particles.[45] For Cu-based oxygen carriers, $MgAl_2O_4$-supported CuO materials have been successfully used as the CLOU oxygen carrier in continuous operation,[17,40] showing complete fuel conversion and high carbon capture efficiency.[40] Although the crushing strength of the fresh particles has been reported above 1 N, their mechanical stability has been found to decrease substantially after 40 h in continuous operation.[34] Nevertheless, the oxygen uncoupling behavior and fuel conversion of these particles was not affected.

The aim of this study is to investigate whether combining different supports of $MgAl_2O_4$, TiO_2, and SiO_2 could potentially increase the mechanical stability of Cu-based oxygen carriers for the CLOU application. The oxygen uncoupling property of these oxygen carriers during N_2 exposure and their reactivity with methane in the temperature range of 900−950 °C has been assessed. In addition, the oxygen carriers have been evaluated in a jet-cup attrition rig with regard to their attrition resistance and mechanical integrity.

2. EXPERIMENTAL SECTION

2.1. Preparation and Fabrication of the Oxygen Carriers. The oxygen carriers prepared in this investigation are summarized in Table 1. The particles were manufactured by spray-drying at VITO (Flemish Institute for Technological Research, Belgium). In this technique, a water-based slurry of CuO (Sigma Aldrich) and the intended combination of support powders of $MgAl_2O_4$ (S30CR, Baikowski), TiO_2 (Alfa Aesar), and SiO_2 (SilverBond M800, Sibelco) were prepared. All particles were prepared to obtain 40 wt % CuO and 60 wt % support material, but the support materials were combined in different ratios of 20/40 wt % (or 40/20 wt %) and 20/20/20 wt %. The powder mixtures were then ball milled, and organic binders were added prior to spray-drying. During continuous stirring, the slurry was pumped through a spray-drying nozzle to form spherical particles which were then injected into the hot spray-drying chamber. After drying and collecting, the fraction between 106 and 212 μm was separated from the rest of the batch by sieving. This was followed by calcination of the material at the selected temperature indicated in Table 1 for 4 h. The calcined material was sieved through stainless steel screens to yield particles in the range of 125−180 μm. It should be mentioned that it was not possible to obtain any materials with a combination of all three supports, i.e. C4AM2T2S2, because the materials melted during calcination, even at lower temperatures. Also, the C4AM2S4 formulation failed because the calcined particles were too soft. It may be possible that the combination of the different supports and the active phase with the given composition resulted in mixtures with a lower melting point than the pure substances. This is a phenomenon common in solid mixtures consisting of different oxides when heat-treated at high temperatures.

2.2. Characterization of the Oxygen Carriers. The crystalline phases of the oxygen carriers were identified using powder X-ray diffraction (Bruker AXS, D8 Advanced) with Cu Kα1 radiation. The bulk (tapped) density was obtained for particles in the size range of 125−180 μm with a graduated cylinder. The Brunauer−Emmett−Teller (BET) specific surface area was determined using N_2-adsorption (Micromeritics, TriStar 3000). The particle size distribution (PSD) was calculated using a light microscope (Nikon, SMZ800) and ImageJ software,[46] which measured the area of an ellipse fitted to a large number of particles. The crushing strength, i.e., the force needed to fracture a single particle, was found by using a digital force gauge (Shimpo, FGN-5) for particles in the size range of 180−250 μm. Thirty measurements were made for every sample, and the average measurement was chosen

as the representative crushing strength. The morphology of the particles was examined with an environmental scanning electron microscope (ESEM) fitted with a field emission gun (FEI, Quanta 200).

The attrition rate of the particles sized 125−180 μm was measured using a customized jet-cup attrition rig,[45] which simulates the effects of grid jet attrition and cyclone attrition in a circulating fluidized-bed combustor. The jet-cup attrition rig consisted of a conical cup located at the bottom of the apparatus with a nozzle that was tangentially introduced in relation to the cup wall. The cup was placed at the bottom of a gravitational particle-gas separator, which was an additional cone. Due to the increasing cross-section area in the upper cone, the gas velocity in the settling chamber was much lower compared to the inlet. Therefore, the low gas velocity in this upper region allowed the elutriated particles to fall back into the cup, while the produced fines were allowed to exit. At the top of the apparatus, a particle filter with a mesh size of 0.01 μm was mounted to collect the fines. Approximately, 5 g of a fresh sample was placed inside the cup, and the apparatus was assembled. Air at 10 L/min was introduced at the nozzle, which corresponds to an air jet velocity of approximately 94 m/s. In order to avoid static electricity, which otherwise would cause particles to adhere to the inner walls of the apparatus, the air was humidified by bubbling it through a column of water. Six measurements at 10 min intervals were made for every sample. These experiments were carried out at room temperature and near atmospheric pressure.[45]

2.3. Experimental Setup and Procedure in the Fluidized-Bed Reactor. A laboratory-scale fluidized-bed reactor system was used for examining the oxygen uncoupling behavior and the reactivity of the oxygen carriers. The scheme of the experimental setup used in this investigation is shown in Figure 2. The dimensions of the quartz reactor

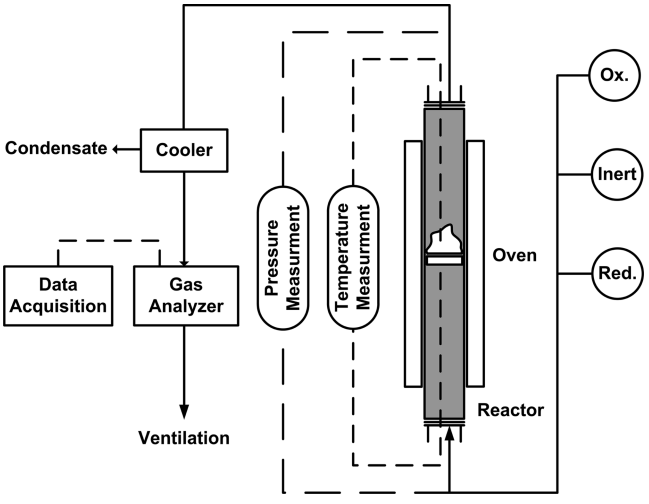

Figure 2. Schematic of the experimental setup used in this investigation.

were as follows: 870 mm high and 22 mm in inner diameter with a porous quartz plate located at a height of 370 mm from the bottom. The reactor temperature was measured with chromel-alumel (type K) thermocouples sheathed in inconel-600 located about 5 mm below and 25 mm above the plate. Pressure transducers (Honeywell) were used to measure the pressure drop over the bed of particles and the quartz plate at a frequency of 20 Hz. The pressure drop over the quartz plate was approximately constant for constant flows. Thus, it was possible to determine if the particles were fluidized or not, by measuring the fluctuations in the pressure drop; i.e., a defluidization would be noted from a decrease in pressure fluctuations. The exit gas stream from the reactor was led into a condenser to remove the water that was generated during the oxidation of the fuel. The composition of the dry gas was measured using a Rosemount NGA-2000 analyzer which measured the concentration of O_2 through a paramagnetic channel and CO_2, CO, and CH_4 through infrared channels with correction for other measured gases.

Fifteen grams of the sample was placed on the porous plate, and the reactor was heated to 900 °C in an 11% O_2−balance N_2 mixture, in order to oxidize the oxygen carrier fully, prior to experiments. In previous investigations using the same experimental setup,[23,47] a 5% O_2 stream was used during the oxidation phase. This was done in order to determine whether the oxygen carrier could be oxidized under oxygen deficient conditions similar to those at the outlet of the air reactor in a realistic CLC unit. The rationale of using an 11% O_2 stream instead, in this study, was to accelerate the oxidation process, particularly at 950 °C, at which point the equilibrium oxygen concentration over CuO−Cu_2O is approximately 4.5%. Hereinafter, the term "cycle" will be used to mean a redox cycle involving the reduction of the oxygen carrier sample in inert gas or fuel, followed by oxidation with the aforementioned 11% O_2 mixture. A set of three inert gas (N_2) cycles was carried out at 900, 925, and 950 °C for 360 s, to investigate the oxygen release. Subsequent to the inert cycles, fuel cycles with 100% methane for 20 s during the reduction period were carried out at 900, 925, and 950 °C. Nitrogen was used as an inert purge for 60 s in between the oxidation and reduction periods. Each cycle was repeated three times to establish reproducibility of the performance. Thus, the performance of the oxygen carriers was evaluated in a total of 18 cycles corresponding to approximately 8 h of operation under hot conditions in the fluidized-bed reactor. Flow rates of 450, 600, and 900 mL_N/min were used during reduction, inert, and oxidation, respectively. These flow rates were chosen to achieve a value of the superficial gas velocity, U, in the reactor approximately 4−12, 8−23, and 13−35 times higher than the calculated minimum fluidization gas velocity, U_{mf}, of the oxygen carrier particles during reduction (with methane), inert, and oxidation periods, respectively. The minimum fluidization velocity, U_{mf}, was calculated by using the correlation given by Kunii and Levenspiel.[48] However, it should be noted that due to gas expansion during reduction, the actual velocity in the bed was higher, as 1 mol of CH_4 was converted to 1 mol of CO_2 and 2 mol of H_2O. There was no carbon deposition during the reduction period, which would have been identified by way of carbon burnoff in the subsequent oxidation period. This was due to the fact that the oxygen available in the oxygen carriers was more than the stoichiometric demand of the fuel.

2.4. Data Analysis. The reactivity of a given oxygen carrier has been quantified in terms of gas yield or conversion efficiency, γ, and has been defined as the fraction of fully oxidized fuel divided by the carbon containing gases in the outlet stream, in this study CO_2, CO, and CH_4.

$$\gamma_{CH_4} = \frac{y_{CO_2}}{y_{CO_2} + y_{CH_4} + y_{CO}} \tag{4}$$

Here, y_i denotes the concentration (vol %) of the respective gas measured with the gas analyzer.

In order to facilitate a comparison between different oxygen carriers at varying temperatures, $\gamma_{CH_4,ave}$, is used, which is defined as the average of gas yield in eq 5 for the entire reduction period.

The mass-based conversion of the oxygen carrier, ω, is defined as

$$\omega = \frac{m}{m_{ox}} \tag{5}$$

where m is the actual mass of the oxygen carrier during the experiments.

Equation 6 is employed for calculating ω as a function of time during the reduction period from the measured concentrations of various gaseous species:

$$\omega_i = 1 - \int_{t_0}^{t_1} \frac{\dot{n}_{out} M_O}{m_{ox}} (4y_{CO_2} + 2y_{O_2} - y_{H_2})\, dt \tag{6}$$

where ω_i is the instantaneous mass-based conversion at time t_1, $\dot{n}_{out}$ is the molar flow rate of the dry gas at the reactor outlet as measured with the analyzer, M_O is the molar mass of oxygen, and t_0 and t_1 are the initial and final times of measurement.

3. RESULTS

3.1. Oxygen Uncoupling of the Carriers. Reduction−oxidation multicycles were carried out in a fluidized-bed reactor

dx.doi.org/10.1021/ef401161s | Energy Fuels 2013, 27, 3918−3927

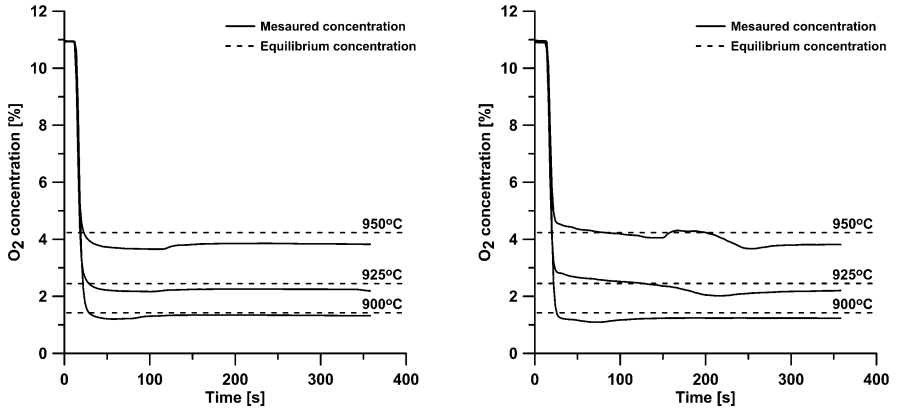

Figure 3. Measured and equilibrium oxygen concentrations during the inert period at different bed temperatures for (left) C4S6_1000 and (right) C4MA4T2_970.

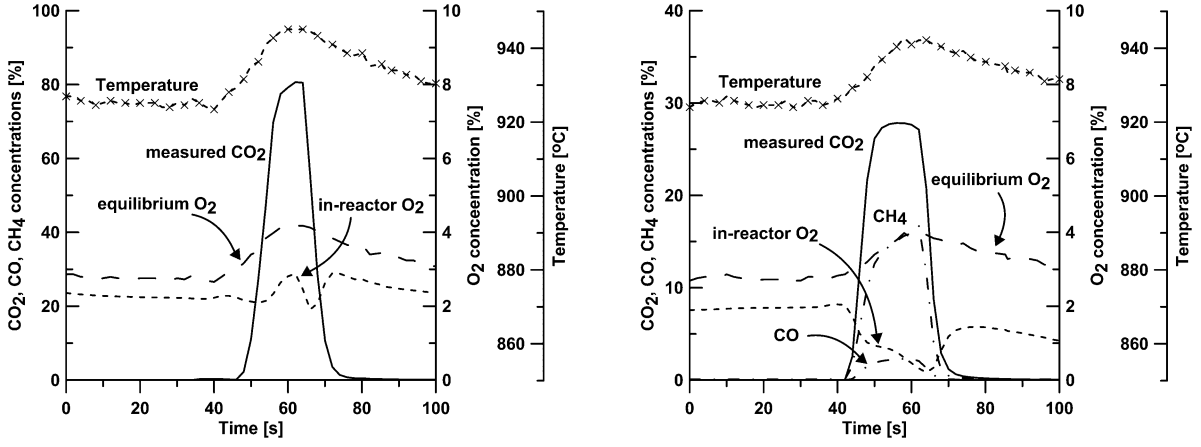

Figure 4. Concentration and temperature profiles for C4MA6_1030 (left) and C4MA4S2_1030 (right) during reduction cycle with methane at 925 °C.

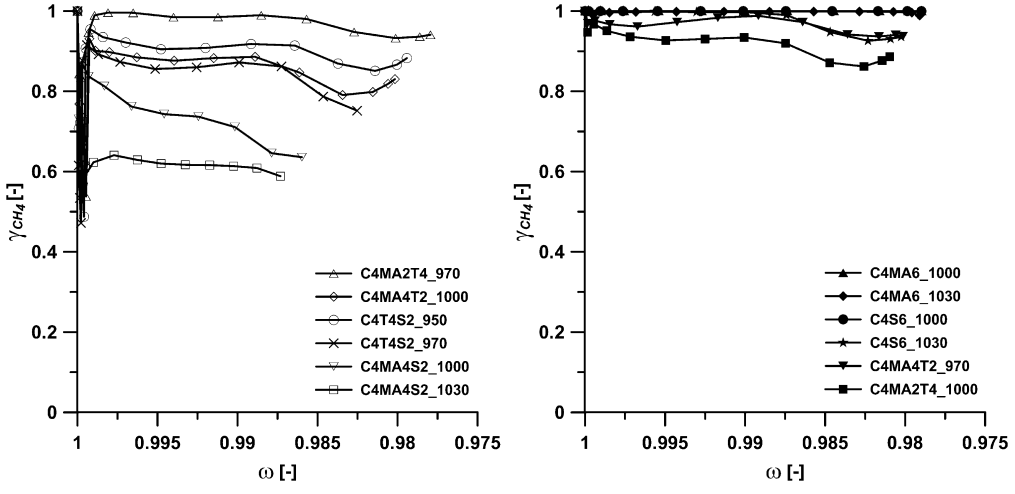

Figure 5. Reactivity (gas yield, γ, νs. mass based conversion, ω) of oxygen carriers with methane as the fuel at 950 °C for oxygen carriers with CS > 1 (left) and oxygen carriers with CS ≤ 1 (right).

to investigate the oxygen release behavior of the oxygen carriers, the reactivity with methane, and the fluidization behavior of the materials with respect to agglomeration and/or defluidization. The oxygen carriers with only TiO_2 (C4T6) and with a combination of 20 wt % TiO_2 and 40 wt % SiO_2 (C4T2S4) as the support agglomerated during the first inert cycle and thus were not further investigated. As an example, Figure 3 shows the oxygen concentration in the outgoing gas from the reactor for the C4S6_1000 and C4MA4T2_970 oxygen carriers and the corresponding equilibrium oxygen concentration at three different temperatures, i.e. 900, 925, and 950 °C. During the inert period, the majority of the oxygen carriers investigated in this study released oxygen close to the corresponding equilibrium concentration at the different temperatures studied.

3.2. Reactivity of the Oxygen Carriers. Figure 4 shows the gas concentration and the temperature profiles during the

dx.doi.org/10.1021/ef401161s | *Energy Fuels* 2013, 27, 3918−3927

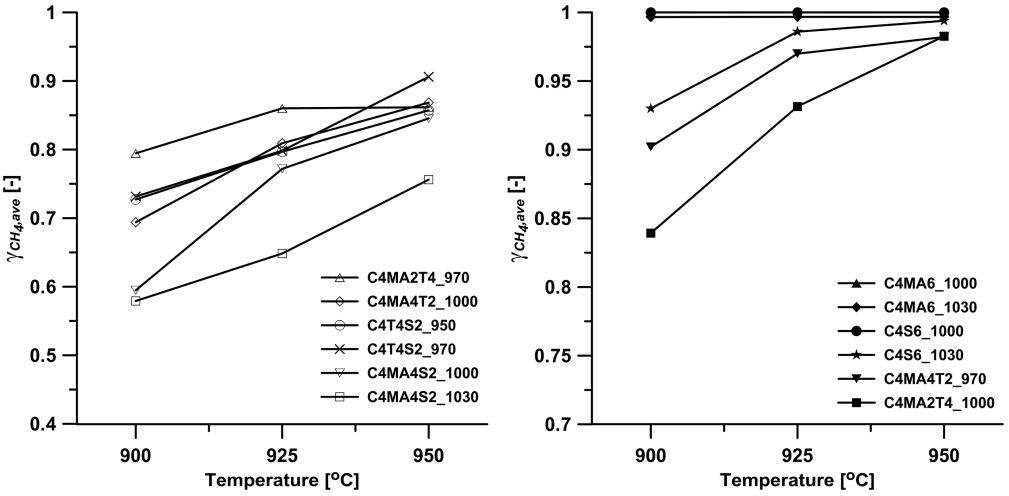

Figure 6. Average gas yield, $\gamma_{CH_4,ave}$, as a function of temperature for oxygen carriers with CS > 1 (left) and oxygen carriers with CS ≤ 1 (right). Note: For reasons of clarity, the scale of $\gamma_{CH_4,ave}$ is different in the figures.

reactivity test with methane at 925 °C for the C4MA6_1030 and C4MA4S2_1030 oxygen carriers. It can be seen that for C4MA6_1030 as the oxygen carrier, Figure 4 (left), there is complete conversion of fuel to CO_2 and H_2O. During reduction, the temperature in the bed increased by approximately 25 °C, and thus the oxygen carrier released more oxygen. This and the complete fuel conversion obtained here are primarily due to the fast rate of oxygen release from this carrier. The high reactivity of the C4MA6_1030 formulation is also in conformity with previous investigations using the $MgAl_2O_4$-supported CuO oxygen carrier.[17,20,23,34,35,40] Subsequent to reduction, the oxygen carrier continued releasing oxygen close to equilibrium concentration. It should be noted that the in-reactor O_2 concentration accounts for the dilution created by water produced during the conversion of methane, which was later removed in the condenser. For C4MA4S2_1030 as the oxygen carrier, Figure 4 (right), there was incomplete conversion of methane and unconverted products, such as CO and CH_4, observed at the reactor's outlet stream. Moreover, during the reduction, the release of O_2 from the oxygen carrier decreased. These effects could be attributed to the much slower rate of oxygen release for this carrier than for the C4MA6_1030 material.

Figure 5 shows the gas yield as a function of the mass-based conversion of all of the investigated oxygen carriers at 950 °C using methane as the fuel for the third repeated cycle. It can be observed that, in general, oxygen carriers with a higher crushing strength, as shown in Figure 5 (left), exhibited a lower reactivity or slower rate of oxygen release than those with a lower crushing strength, as illustrated in Figure 5 (right). Thus, most of the oxygen carriers with a crushing strength of 1 or lower exhibited close to complete conversion of the fuel. For instance, oxygen carriers prepared with only $MgAl_2O_4$ (C4MA6) or SiO_2 (C4S6) as the support showed the highest reactivity during methane conversion with γ close to 1 and a change in the mass-based conversion, ω, of the carriers of approximately 2%. However, when mixtures of these supports were used (C4MA4S2), the reactivity of the oxygen carriers decreased substantially. It may be possible that the addition of SiO_2 resulted in lowered gas diffusion in the oxygen carriers in comparison to their counterparts with single-phase supports. However, this was not the case for oxygen carriers based on $MgAl_2O_4/TiO_2$ (C4MA2T4_970 and C4MA4T2_1000) and TiO_2/SiO_2 (C4T4S2) as the support. Despite having crushing strengths higher than 1, the latter oxygen carriers also showed reasonably high fuel conversion with γ higher than 0.9 and a change in the mass-based conversion, ω, of the carriers of approximately 2%.

Figure 6 shows the average gas yield, $\gamma_{CH_4,ave}$, as a function of temperature for the investigated oxygen carriers that used methane as the fuel and for the third repeated cycle. It can be observed that for most of the oxygen carriers, the average gas yield for methane rose with the temperature, likely due to a faster rate of oxygen release at higher temperatures. Table 2 summarizes the overall functionality of the oxygen carriers

Table 2. Overall Functionality of the Oxygen Carriers during the Reactivity Tests

oxygen carrier	agglomeration during inert cycles	oxygen concentration during inert gas periods	gas conversion
C4T6_950	yes		
C4T6_970	yes		
C4MA6_1000	no	very close to equilibrium	very high
C4MA6_1030	no	very close to equilibrium	very high
C4S6_1000	no	very close to equilibrium	very high
C4S6_1030	no	very close to equilibrium	very high
C4MA4T2_970	no	slightly lower than equilibrium	high
C4MA4T2_1000	no	slightly lower than equilibrium	high
C4MA2T4_970	no	slightly lower than equilibrium	high
C4MA2T4_1000	no	slightly lower than equilibrium	high
C4MA4S2_1000	no	lower than equilibrium	average
C4MA4S2_1030	no	lower than equilibrium	average
C4T4S2_950	no	slightly lower than equilibrium	high
C4T4S2_970	no	slightly lower than equilibrium	high
C4T2S4_1000	yes		
C4T2S4_1030	yes		

dx.doi.org/10.1021/ef401161s | *Energy Fuels* 2013, 27, 3918−3927

Table 3. Physical and Chemical Properties and Characteristics of the Tested Oxygen Carriers As Prepared and Used

	bulk density [g/cm^3][a]			BET specific surface area [m^2/g][a]			
oxygen carrier	fresh	trend	used	fresh	trend	used	crystalline phases detected by XRD
C4MA6_1000	0.97	↓	0.80	8.81	↓	7.99	CuO, $MgAl_2O_4$
C4MA6_1030	1.03	↓	0.79	7.05	–	7.09	
C4S6_1000	0.93	–	0.91	1.10	↑	1.58	CuO, SiO_2 (quartz), SiO_2 (cristobalite)
C4S6_1030	0.96	↓	0.88	0.71	–	0.71	
C4MA4T2_970	1.54	↓	1.34	0.21	↑	0.67	$MgAl_2O_4$, $MgTi_2O_5$, CuO
C4MA4T2_1000	1.71	↓	1.30	0.04	↑	0.67	
C4MA2T4_970	1.55	↓	1.30	0.25	↑	0.74	$MgAl_2O_4$, TiO_2, CuO, $MgTi_2O_5$
C4MA2T4_1000	1.54	↓	1.18	0.04	↑	0.58	
C4MA4S2_1000	1.67	↓	1.10	0.25	↑	0.68	$CuMgSi_2O_6$, CuO, $MgAl_2O_4$
C4MA4S2_1030	1.66	↓	1.15	0.16	↑	0.77	
C4T4S2_950	1.81	↓	1.46	0.38	–	0.35	CuO, TiO_2, SiO_2 (tridymite), SiO_2 (quartz)
C4T4S2_970	1.93	↓	1.44	0.04	↑	0.22	

[a]The mean particle size in the measurement of bulk density and BET specific area was approximately 152.5 μm.

during the inert gas and reactivity cycles. For oxygen carriers with high rates of oxygen release, i.e., those reaching closer to equilibrium concentration of oxygen, the methane conversion was most likely dominated by the CLOU mechanism. However, for oxygen carriers with a lower rate of oxygen release, i.e., in which the oxygen concentration was considerably lower than the equilibrium concentration, the CLC mechanism was dominant.

3.3. Attributes of the Oxygen Carriers before and after Reactivity Tests. Table 3 summarizes the study of oxygen carrier particles with respect to the physical and chemical changes that these materials undergo during the redox processes. For the majority of the samples, there was a decrease in the density and an increase in the BET specific surface area of the particles. However, there was no change in the crystalline phase of any of the oxygen carriers after the reactivity test compared to their fresh counterparts, as determined with the XRD analysis. Figure 7 shows the XRD signatures of fresh as well as used samples for C4MA4S2_1000 and C4MA4T2_1000 as an example. It should be mentioned that in the case of the used samples, the reactivity cycles were ended with an oxidation (11% O_2) stream. In the case of C4MA4S2_1000, it could be observed that the active CuO phase had reacted with both the $MgAl_2O_4$ and the SiO_2 support phases, which resulted in the formation of $CuMgSi_2O_6$. This could result in an oxygen carrier conversion lower than theoretically expected, should the $CuMgSi_2O_6$ be unreactive. In the case of the $MgAl_2O_4/TiO_2$ as the support, an interaction could be seen between the supports, which resulted in the formation of $MgTi_2O_5$.

Some of the oxygen carriers prepared here showed reasonable mechanical stability, as indicated by the crushing strength measured prior to the reactivity tests shown in Table 1. It should be noted that the crushing strength might not correlate linearly with attrition and fragmentation behavior in a real CLC system. Dust formation or particle fragmentation was not observed for any of the particles after the reactivity tests. However, given that the total number of cycles and the gas velocities employed in this study were rather low, further long-term tests in continuous operation will be needed in order to confirm the mechanical stability of these materials. Figure 8 shows the rate of attrition of the fresh oxygen carriers during testing in a jet-cup attrition rig for 1 h. In Table 4, the attrition index, A_i, defined as the slope of the attrition in the last 30 min of the test period, is shown for the investigated oxygen carriers. It can be seen that, except for the C4S6 materials, which had high attrition rates and turned into dust, the rest of the oxygen carriers had very similar attrition

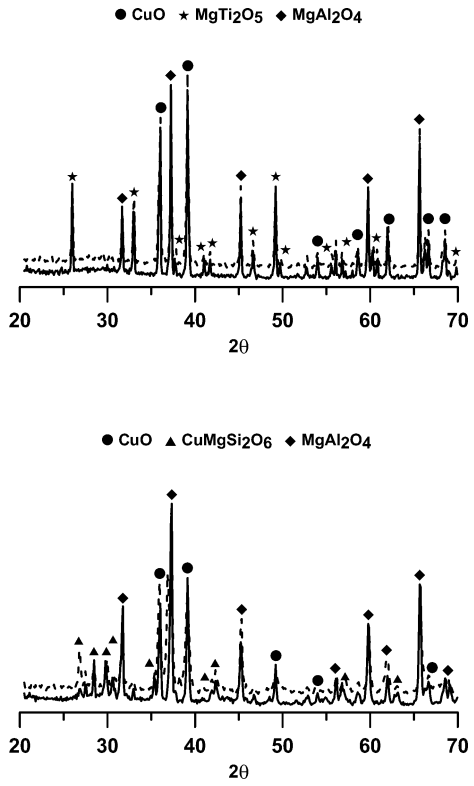

Figure 7. Comparative XRD signatures of fresh and used oxygen carriers for (top) C4MA4T2_1000 and (bottom) C4MA4S2_1000. Solid lines represent fresh and dashed lines represent materials after the reactivity test.

rates. The attrition rates of the materials used here are much lower than previously investigated spray-dried Cu-based oxygen carriers[45] with ZrO_2 as the support, which were tested in the same apparatus and had shown reasonable functionality in continuous operation in a 300 W reactor.[41] Therefore, the combination of supports has indeed resulted in the formation of oxygen carriers with high mechanical resistance while maintaining sufficiently high reactivity and oxygen release ability for the CLOU application. The attrition rates for the oxygen carriers prepared with $MgAl_2O_4/TiO_2$, $MgAl_2O_4/SiO_2$, and TiO_2/SiO_2 as the support are comparable to those for $CaMn_{0.9}Mg_{0.1}O_{3-\delta}$, which has shown excellent functionality in continuous operation in a 10 kW unit.[49] Thus, equally good results could be expected

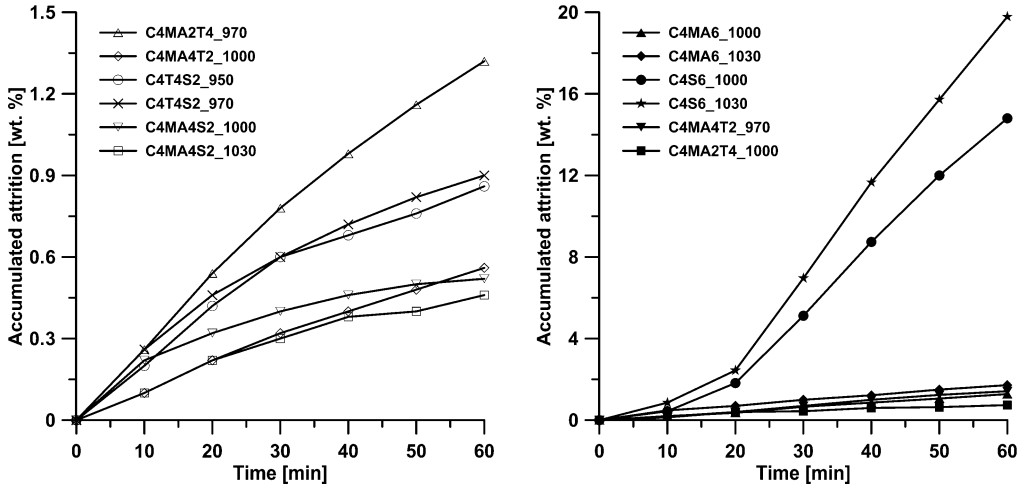

Figure 8. Accumulated attrition as a function of time for oxygen carriers with CS > 1 (left) and (b) CS ≤ 1 (right). Note: For reasons of clarity, the scale of accumulated attrition is different in the figures.

Table 4. Attrition Rates of the Tested Oxygen Carriers and Their Corresponding Crushing Strength (CS) in the Fresh State

oxygen carrier	attrition rate, A_i [wt %/h]	crushing strength (CS) [N]
C4MA6_1000	1.2	0.6
C4MA6_1030	1.4	0.8
C4S6_1000	19.4	0.7
C4S6_1030	25.6	0.5
C4MA4T2_970	1.4	1.0
C4MA4T2_1000	0.5	1.5
C4MA2T4_970	1.1	1.3
C4MA2T4_1000	0.6	1.0
C4MA4S2_1000	0.2	1.4
C4MA4S2_1030	0.3	1.7
C4T4S2_950	0.5	1.7
C4T4S2_970	0.6	1.8

for these materials; nevertheless, experiments in continuous operation are required for confirmation.

The particle size distribution (PSD) of the oxygen carriers before and after the reactivity test for particles with an attrition rate below 1 wt %/h are shown in Figure 9. It can be seen that these materials exhibit an overall increase in particle size for these materials. This factor, together with the decrease in density and the increase in BET specific surface area of the particles (Table 4), indicates that the majority of the oxygen carriers investigated here experienced some degree of swelling during the reactivity tests.

The ESEM images of the fresh and used C4T4S2_950 oxygen carrier are shown in Figure 10, as an example. The porosity of the particles seems to have increased after the reactivity test compared to the fresh samples. This was the case for most of the oxygen carriers investigated here. Thus, the slight increase in size distribution shown in Figure 9 is most likely associated with the increase in the porosity of the particles. Similar observations have been made previously for $MgAl_2O_4$-supported CuO materials after reactivity tests.[23,34]

Figure 11 shows the average gas yield, $\gamma_{CH_4,ave}$, at 925 °C for the investigated oxygen carriers, as a function of their attrition rate, A_i. It can be observed that oxygen carriers with a higher gas yield are also more prone to attrition. Thus, there may be a trade-off between the reactivity of the oxygen carriers and their resistance

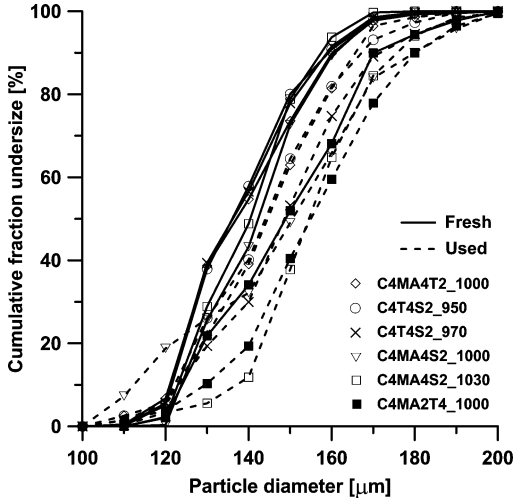

Figure 9. Particle size distributions (PSD) of fresh and used oxygen carriers, with attrition rate, A_i, less than 1 wt %/h.

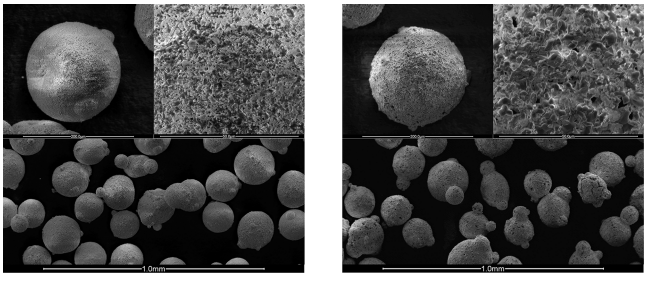

Figure 10. ESEM images of (left) fresh and (right) used C4T4S2_950 particles after the reactivity tests. The size bars for the images with higher magnification are 200 and 50 μm, while those of the images with lower magnification are 1 mm.

to attrition. For application in a full scale plant, oxygen carriers with high attrition resistance are required, as they will be circulated for many cycles. In particular, C4MA2T4_1000 features high reactivity, CLOU behavior, and a low attrition rate. The C4MA4S2 materials achieve the lowest attrition rates but remain fairly reactive.

dx.doi.org/10.1021/ef401161s | *Energy Fuels* 2013, 27, 3918−3927

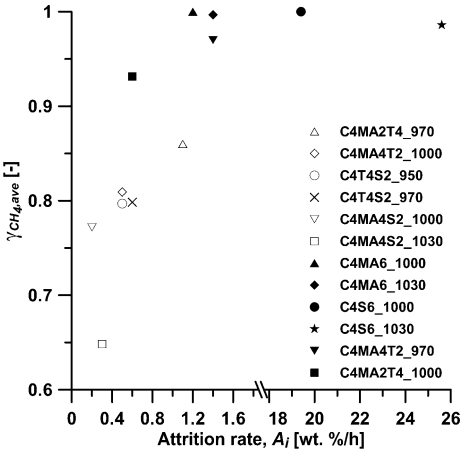

Figure 11. Average gas yield, $\gamma_{CH_4,ave}$, at 925 °C as a function of attrition rate, A_i, for the investigated oxygen carriers.

4. CONCLUSION

Several oxygen carriers based on CuO as the active phase and a combination of $MgAl_2O_4$, SiO_2, and TiO_2 as the support were investigated for the CLOU application. The particles were prepared by spray drying, and the experiments were carried out in a fluidized-bed batch reactor in the temperature range of 900−950 °C. Their CLOU behavior was assessed in an N_2 environment, and their reactivity was tested with methane. Most of the oxygen carriers exhibited oxygen uncoupling behavior reaching that reached close to the equilibrium concentration of oxygen over CuO/Cu_2O, at the corresponding experimental temperature. In terms of methane conversion, oxygen carriers with a crushing strength below 1 generally had a higher rate of oxygen release and higher fuel conversion. However, by combining different supports, it was possible to obtain oxygen carriers with high mechanical stability, with oxygen release behavior and high reactivity with methane.

On the basis of the results from the reactivity and jet-cup attrition rig experiments, oxygen carriers prepared with $MgAl_2O_4/TiO_2$, $MgAl_2O_4/SiO_2$, and TiO_2/SiO_2 as the support exhibited a combination of high mechanical stability, low attrition rates, good reactivity with methane, and oxygen uncoupling behavior.

AUTHOR INFORMATION

Corresponding Author

*Telephone: +46-31-772-2822. E-mail: arjmand@chalmers.se.

Notes

The authors declare no competing financial interest.

ACKNOWLEDGMENTS

I.A.-R. thanks CSIC for the JAE fellowship cofunded by the European Social Fund and the project PN-ENE2010-19550 supported by the Spanish Ministry of Science and Innovation. The authors also wish to acknowledge Vattenfall and Chalmers University of Technology via the Energy Area of Advance for the financial support for this study.

REFERENCES

(1) Pachauri, R. K.; Reisinger, A. *Fourth Assesment Report: Climate Change (Synthesis Report)*; Intergovernmental Panel on Climate Change: Geneva, 2007.

(2) Herzog, H. J. CO_2 capture and storage: Costs and market potential. In *Greenhouse Gas Control Technologies 7*; Rubin, E. S., Keith, D. W., Gilboy, C. F., Wilson, M., Morris, T., Gale, J., Thambimuthu, K., Thambimuthu, K., Eds.; Elsevier Science Ltd: Oxford, 2005; pp 21−28.

(3) Lyngfelt, A.; Leckner, B.; Mattisson, T. A fluidized-bed combustion process with inherent CO_2 separation; application of chemical-looping combustion. *Chem. Eng. Sci.* **2001**, *56* (10), 3101−3113.

(4) Ishida, M.; Jin, H. A Novel Chemical-Looping Combustor without NO_x Formation. *Ind. Eng. Chem. Res.* **1996**, *35* (7), 2469−2472.

(5) Kronberger, B.; Johansson, E.; Löffler, G.; Mattisson, T.; Lyngfelt, A.; Hofbauer, H. A Two-Compartment Fluidized Bed Reactor for CO_2 Capture by Chemical-Looping Combustion. *Chem. Eng. Technol.* **2004**, *27* (12), 1318−1326.

(6) Jerndal, E.; Mattisson, T.; Lyngfelt, A. Thermal Analysis of Chemical-Looping Combustion. *Chem. Eng. Res. Des.* **2006**, *84* (9), 795−806.

(7) Lewis, K. W.; Gilliland, E. R.; Sweeney, M. P. Gasification of Carbon Metal Oxides in a Fluidized Powder Bed. *Chem. Eng. Prog.* **1951**, *47* (5), 251−256.

(8) Ishida, M.; Jin, H. A new advanced power-generation system using chemical-looping combustion. *Energy* **1994**, *19* (4), 415−422.

(9) Lyngfelt, A.; Thunman, H. Construction and 100 h of operational experience of a10 kW chemical looping combustor. In *The CO_2 Capture and Storage Project (CCP) for Carbon Dioxide Storage in Deep Geologic Formations For Climate Change Mitigation*; Thomas, D., Ed.; Elsevier Science: London, 2003; Vol. *1*—Capture and Separation of Carbon Dioxide From Combustion Sources.

(10) Kolbitsch, P.; Pröll, T.; Bolhar-Nordenkampf, J.; Hofbauer, H. Design of a Chemical Looping Combustor using a Dual Circulating Fluidized Bed (DCFB) Reactor System. *Chem. Eng. Technol.* **2009**, *32* (3), 398−403.

(11) Lyngfelt, A. Oxygen Carriers for Chemical Looping Combustion - 4000 h of Operational Experience. *Oil Gas Sci. Technol.* **2011**, *66* (2), 161−172.

(12) Lyngfelt, A.; Mattisson, T. Materials for Chemical-Looping Combustion. *Efficient Carbon Capture for Coal Power Plants*; Stolten, D., Sherer, V., Eds.; WILEY-VCH Verlag GmbH & Co. KGaA: Weinheim, Germany, 2011; Chapter 17.

(13) Hossain, M. M.; de Lasa, H. I. Chemical-looping combustion (CLC) for inherent CO_2 separations-a review. *Chem. Eng. Sci.* **2008**, *63* (18), 4433−4451.

(14) Adanez, J.; Abad, A.; Garcia-Labiano, F.; Gayan, P.; de Diego, L. F. Progress in Chemical-Looping Combustion and Reforming technologies. *Prog. Energy Combust. Sci.* **2012**, *38* (2), 215−282.

(15) Scott, S. A.; Dennis, J. S.; Hayhurst, A. N.; Brown, T. In situ gasification of a solid fuel and CO_2 separation using chemical looping. *AIChE J.* **2006**, *52* (9), 3325−3328.

(16) Mattisson, T.; Lyngfelt, A.; Leion, H. Chemical-looping with oxygen uncoupling for combustion of solid fuels. *Int. J. Greenhouse Gas Control* **2009**, *3* (1), 11−19.

(17) Abad, A.; Adánez-Rubio, I.; Gayán, P.; García-Labiano, F.; de Diego, L. F.; Adánez, J. Demonstration of chemical-looping with oxygen uncoupling (CLOU) process in a 1.5 kW_{th} continuously operating unit using a Cu-based oxygen-carrier. *Int. J. Greenhouse Gas Control* **2012**, *6*, 189−200.

(18) Gayán, P.; Adánez-Rubio, I.; Cuadrat, A.; Mendiara, T.; Abad, A.; García-Labiano, F.; De Diego, L.; Adánez, J. Use of Chemical-Looping processes for coal combustion with CO_2 capture. *Energy Procedia* **2013**, In Press.

(19) Arjmand, M.; Keller, M.; Leion, H.; Mattisson, T.; Lyngfelt, A. Oxygen Release and Oxidation Rates of $MgAl_2O_4$-Supported CuO Oxygen Carrier for Chemical-Looping Combustion with Oxygen Uncoupling (CLOU). *Energy Fuels* **2012**, *26* (11), 6528−6539.

(20) Adánez-Rubio, I.; Abad, A.; Gayán, P.; de Diego, L. F.; García-Labiano, F.; Adánez, J. Identification of operational regions in the Chemical-Looping with Oxygen Uncoupling (CLOU) process with a Cu-based oxygen carrier. *Fuel* **2012**, *102*, 635−645.

(21) Chuang, S. Y.; Dennis, J. S.; Hayhurst, A. N.; Scott, S. A. Development and performance of Cu-based oxygen carriers for

chemical-looping combustion. *Combust. Flame* **2008**, *154* (1−2), 109−121.
(22) Dennis, J. S.; Müller, C. R.; Scott, S. A. In situ gasification and CO_2 separation using chemical looping with a Cu-based oxygen carrier: Performance with bituminous coals. *Fuel* **2010**, *89* (9), 2353−2364.
(23) Arjmand, M.; Azad, A.-M.; Leion, H.; Lyngfelt, A.; Mattisson, T. Prospects of Al_2O_3 and $MgAl_2O_4$-Supported CuO Oxygen Carriers in Chemical-Looping Combustion (CLC) and Chemical-Looping with Oxygen Uncoupling (CLOU). *Energy Fuels* **2011**, *25* (11), 5493−5502.
(24) Forero, C. R.; Gayán, P.; García-Labiano, F.; de Diego, L. F.; Abad, A.; Adánez, J. High temperature behaviour of a $CuO/\gamma Al_2O_3$ oxygen carrier for chemical-looping combustion. *Int. J. Greenhouse Gas Control* **2011**, *5* (4), 659−667.
(25) Gayán, P.; Forero, C. R.; Abad, A.; de Diego, L. F.; García-Labiano, F.; Adánez, J. Effect of Support on the Behavior of Cu-Based Oxygen Carriers during Long-Term CLC Operation at Temperatures above 1073 K. *Energy Fuels* **2011**, *25* (3), 1316−1326.
(26) Mattisson, T.; Järdnäs, A.; Lyngfelt, A. Reactivity of Some Metal Oxides Supported on Alumina with Alternating Methane and Oxygen Application for Chemical-Looping Combustion. *Energy Fuels* **2003**, *17* (3), 643−651.
(27) de Diego, L. F.; Gayán, P.; García-Labiano, F.; Celaya, J.; Abad, A.; Adánez, J. Impregnated CuO/Al_2O_3 Oxygen Carriers for Chemical-Looping Combustion: Avoiding Fluidized Bed Agglomeration. *Energy Fuels* **2005**, *19* (5), 1850−1856.
(28) de Diego, L. F.; García-Labiano, F.; Gayán, P.; Celaya, J.; Palacios, J. M.; Adánez, J. Operation of a 10 kWth chemical-looping combustor during 200 h with a $CuO\text{-}Al_2O_3$ oxygen carrier. *Fuel* **2007**, *86* (7−8), 1036−1045.
(29) Arjmand, M.; Azad, A.-M.; Leion, H.; Mattisson, T.; Lyngfelt, A. Evaluation of $CuAl_2O_4$ as an Oxygen Carrier in Chemical-Looping Combustion. *Ind. Eng. Chem. Res.* **2012**, *51* (43), 13924−13934.
(30) Wang, B.; Zhao, H.; Zheng, Y.; Liu, Z.; Yan, R.; Zheng, C. Chemical looping combustion of a Chinese anthracite with Fe_2O_3-based and CuO-based oxygen carriers. *Fuel Process. Technol.* **2012**, *96* (0), 104−115.
(31) de Diego, L. F.; García-Labiano, F.; Adánez, J.; Gayán, P.; Abad, A.; Corbella, B. M.; María Palacios, J. Development of Cu-based oxygen carriers for chemical-looping combustion. *Fuel* **2004**, *83* (13), 1749−1757.
(32) Chuang, S. Y.; Dennis, J. S.; Hayhurst, A. N.; Scott, S. A. Kinetics of the chemical looping oxidation of H_2 by a co-precipitated mixture of CuO and Al_2O_3. *Chem. Eng. Res. Des.* **2011**, *89* (9), 1511−1523.
(33) Mattisson, T.; Leion, H.; Lyngfelt, A. Chemical-looping with oxygen uncoupling using CuO/ZrO_2 with petroleum coke. *Fuel* **2009**, *88* (4), 683−690.
(34) Adánez-Rubio, I.; Gayán, P.; Abad, A.; de Diego, L. F.; García-Labiano, F.; Adánez, J. Evaluation of a Spray-Dried $CuO/MgAl_2O_4$ Oxygen Carrier for the Chemical Looping with Oxygen Uncoupling Process. *Energy Fuels* **2012**, *26* (5), 3069−3081.
(35) Gayán, P.; Adánez-Rubio, I.; Abad, A.; de Diego, L. F.; García-Labiano, F.; Adánez, J. Development of Cu-based oxygen carriers for Chemical-Looping with Oxygen Uncoupling (CLOU) process. *Fuel* **2012**, *96*, 226−238.
(36) Arjmand, M.; Leion, H.; Mattisson, M.; Lyngfelt, A. ZrO_2-Supported CuO Oxygen Carriers for Chemical-Looping with Oxygen Uncoupling (CLOU). *Energy Procedia* **2013**, In press.
(37) Arjmand, M.; Azad, A.-M.; Leion, H.; Rydén, M.; Mattisson, M. $CaZrO_3$ and $SrZrO_3$-supported CuO Oxygen Carriers for Chemical-looping with Oxygen Uncoupling (CLOU). *Energy Procedia* **2013**, In press.
(38) Leion, H.; Mattisson, T.; Lyngfelt, A. Using chemical-looping with oxygen uncoupling (CLOU) for combustion of six different solid fuels. *Energy Procedia* **2009**, *1* (1), 447−453.
(39) Hedayati, A.; Azad, A.-M.; Rydén, M.; Leion, H.; Mattisson, T. Evaluation of Novel Ceria-Supported Metal Oxides As Oxygen Carriers for Chemical-Looping Combustion. *Ind. Eng. Chem. Res.* **2012**, *51* (39), 12796−12806.
(40) Adánez-Rubio, I.; Abad, A.; Gayán, P.; de Diego, L. F.; García-Labiano, F.; Adánez, J. Performance of CLOU process in the combustion of different types of coal with CO_2 capture. *Int. J. Greenhouse Gas Control* **2013**, *12* (0), 430−440.
(41) Moldenhauer, P.; Rydén, M.; Mattisson, T.; Lyngfelt, A. Chemical-looping combustion and chemical-looping with oxygen uncoupling of kerosene with Mn- and Cu-based oxygen carriers in a circulating fluidized-bed 300W laboratory reactor. *Fuel Process. Technol.* **2012**, *104* (0), 378−389.
(42) Xu, L.; Wang, J.; Li, Z.; Cai, N. Experimental Study of Cement-Supported CuO Oxygen Carriers in Chemical Looping with Oxygen Uncoupling (CLOU). *Energy Fuels* **2013**, *27* (3), 1522−1530.
(43) Eyring, E. M.; Konya, G.; Lighty, J. S.; Sahir, A. H.; Sarofim, A. F.; Whitty, K. Chemical Looping with Copper Oxide as Carrier and Coal as Fuel. *Oil Gas Sci. Technol.* **2011**, *66* (2), 209−221.
(44) Wen, Y.-y.; Li, Z.-s.; Xu, L.; Cai, N.-s. Experimental Study of Natural Cu Ore Particles as Oxygen Carriers in Chemical Looping with Oxygen Uncoupling (CLOU). *Energy Fuels* **2012**, *26*, 3919−3927.
(45) Rydén, M.; Moldenhauer, P.; Lindqvist, S.; Mattisson, M.; Lyngfelt, A. Measuring attrition resistance of oxygen carrier particles for chemical-looping combustion with the jet cup method. Submitted for publication, 2012.
(46) Rasband, W. S. *ImageJ*; National Institutes of Health: Bethesda, MD, 1997.
(47) Arjmand, M.; Hedayati, A.; Azad, A.-M.; Leion, H.; Rydén, M.; Mattisson, T. $Ca_xLa_{1-x}Mn_{1-y}M_yO_{3-\delta}$ (M = Mg, Ti, Fe, or Cu) as Oxygen Carriers for Chemical-Looping with Oxygen Uncoupling (CLOU). *Energy Fuels* **2013**, DOI: 10.1021/ef3020102.
(48) Kunii, D.; Levenspiel, O. *Fluidization Engineering*; Butterworth-Heinemann: Boston, 1991.
(49) Källén, M.; Rydén, M.; Dueso, C.; Mattisson, T.; Lyngfelt, A. $CaMn_{0.9}Mg_{0.1}O_{3-\delta}$ as Oxygen Carrier in a Gas-Fired 10 kW_{th} Chemical-Looping Combustion Unit. *Ind. Eng. Chem. Res.* **2013**, In press.